Automatic brain tumor segmentation from magnetic resonance images using superpixel-based approach

Muhammad Javaid Iqbal[1] · Usama Ijaz Bajwa[2] · Ghulam Gilanie[3] ·
Muhammad Aksam Iftikhar[2] · Muhammad Waqas Anwar[2]

Abstract

Cancer is the second leading cause of deaths worldwide, reported by World Health Organization (WHO). The abnormal growth of cells, which should die at the time but they remained in body organ which makes tumor and brain tumor is one of them. During its treatment planning, brain tumor segmentation plays its vital role, Magnetic Resonance Imaging (MRI) is most widely used medical imaging modalities to scan brain tissues, and segmentation of brain tumor from MRI scans is still a challenging task, due to the variability in spatial, structure and appearance of the brain tumor. The existing brain tumor segmentation techniques are still suffering from an inadequate performance, dependent on initial assumptions, and required manual interference. The main challenge is to segment out the accurate tumor from MRI images, and to give the solution for its variability in size due to spatial change in image slices. The proposed model in an automated manners segment out abnormal tissues from MRI images. The proposed model has some aspects like we apply some pre-processing techniques, and apply superpixel-

✉ Usama Ijaz Bajwa
  usamabajwa@cuilahore.edu.pk

  Muhammad Javaid Iqbal
  javaid.ciit@gmail.com

  Ghulam Gilanie
  ghulam.gilanie@iub.edu.pk

  Muhammad Aksam Iftikhar
  aksamiftikhar@cuilahore.edu.pk

  Muhammad Waqas Anwar
  waqasanwar@cuilahore.edu.pk

¹ Department of Computer Science and Information Technology, The Superior University, Lahore, Pakistan

² Department of Computer Science, COMSATS University Islamabad, Lahore Campus. 1.5 KM Defence Road off Raiwind Road, Lahore, Pakistan

³ Department of Artificial Intelligence, The Islamia University of Bahawalpur, Bahawalpur, Pakistan

segmentation with their improved tuned parameter values. We have extracted different features for the superpixels in the images such that statistical features, fractal features, texton features, curvature feature and SIFT features. Due to unbalanced feature vector, we have proposed class balancing algorithm, and then apply SVM, KNN, Decision Tree and Ensemble classifiers, to classify the normal and abnormal superpixels. To evaluate the proposed model, we used MICCAI BRATS-2017 MRI training dataset. The Dice Coefficient (DSC), precision, sensitivity, and balanced error rate (BER) against the ground truths for FLAIR sequence in LGG volumes have been obtained as 0.8593, 87%, 93%, and 0.08 respectively. The DSC, precision, sensitivity, and BER against the ground truths for FLAIR sequence in HGG volumes have been obtained as 0.8528, 87%, 97%, and 0.08 respectively. It is evident from the quantitative and visual results that the proposed model provides a close match to the expert delineation for the FLAIR sequence.

1 Introduction

Globally, cancer is the second leading cause of deaths specially in middle and low-income countries. In the year 2020, it was accounted 10 million deaths[1], which are approximately 1 in 6 of all the global deaths [8]. Cancer is the abnormal growth of cells that can spread rapidly to any body organ [8]. These cancerous cells due to abnormal growth combined at any location in the body organ or collection of abnormal cells in body organ become tumor. These tumors affect body organ very badly and same in the case with brain tumor. It can affect almost anybody organ, which has many anatomic and molecular subtypes. Accurate detection of cancerous cells or tumor is central to effective disease prognosis. Early detection can significantly increase the chances of successful treatment.

Various techniques working for segmenting the tumor from the body organ. On other side medical imaging is playing an important role for cancerous cells diagnosis and tumor segmentation. In the medical analysis the most common modalities [7] nowadays are Magnetic Resonance Images (MRI), Computer Tomography (CT Scan), Ultrasound [9] using on large scale, specifically for brain tumor detection, classification and grading. MRI is preferred over other modalities, because of its non-invasiveness property and using radio waves that didn't affect the sensitive body organs like brain. MRI has different sequences like T1-w, T2-w, FLAIR, T1c, PD, T1Ce, and DTI [11]. Can visualize the structure of the brain in all possible planes such as axial views, sagittal views, and coronal views [12], where we can examine the brain in 3D view.

Three different types of brain tumor segmentations are performing in the clinical environment, i.e., manual, semi-automated, and fully- automated segmentation. Manual segmentation although more reliable because radiologist examine themselves, however, it requires major human involvement to identify the tumor regions in brain MRI [3]. Manual method takes time to analyze the large volume patients and somehow found human errors during the examination due to negligence or time factors, that's why it is the best approach to use in practical application only for few patients. Semi-automatic method required initial input to start the

---

[1] https://www.who.int/news-room/fact-sheets/detail/cancer.

process and then system continue to segment out from the MRI images. Whereas, fully automatic require minimum input to perform segmentation, and there is no need for any human efforts. Using this approach, we can easily examine large volume patients in very short time as compared to other two mentioned approaches.

Ramy A. Zeineldin et al. [29] proposed a neural network for brain tumor segmentation, where this study address the crucial problem to distinguish tumor boundaries with healthy cells. It is based on decoupling modular framework, which has two important parts, which consists of the encoder and decoder relationship. To extract the spatial information for the images used convolutional neural network (CNN). To get the complete resolution map, the resulting semantic map pushed towards the decoder. This framework has been introduced on the basis of modified U-net architecture, and other CNN models including ResNet, DensNet, and NASNet. MICCAI BARTS 2019 dataset has been used for evaluation and Dice Coefficient & Hausdorff values are used as standard evaluation measures. The evaluation obtained for this research study in Dice and Hausdorf are 0.81 to 0.84 and 9.8 to 19.7 respectively. LING TAN et al. [27] proposed model for the segmentation of tumor in MRI, which was based on the ACU-Net network. They choose the deep separable convolutional layer for distinguishing the spatial correlation and appearance correlation of the mapped convolutional channel. Further, they replaced the ordinary architecture in the U-Net. The propagation capacity of the features was highlighted in the ACU-Net network by introducing the residual skip connection. To identify the image contour and edge cracks, the active contour model was used for the tumor segmentation.

Early tumor detection and segmentation is the need of time because it helps in early diagnosis, and treatment planning. Tiejun Yang et al. [28] highlight the brain tumor crucial problem such that structural diversity, and low segmentation accuracy. An automatic brain tumor segmentation method proposed with SK-TPCNN (Small Kernels Two Path Convolutional Neural Network) and RF (Random Forest) algorithm for classification. Feature extraction techniques and joint optimization techniques are introduced clearly in this research study. Basically SK-TPCNN joins the small and large convolutional kernels to safe from over fitting and to enhance the non-linear ability. At the end features that are learned pass to the RF classifier which classify between normal and tumorous images. The proposed model evaluated using BRATS 2015 training dataset and obtained 0.86 DSC values in whole tumor or edema.

Kadkhodaei et al. [15] proposed a technique to address the brain tumor segmentation issues in variation of tumor size, shape and appearance properties. They proposed the technique in which they map all MRI images on the same scale. After scaling, they enhanced and normalize the dataset, enhanced images were then segment out using 3D super voxel approach including saliency algorithm and edge-aware filtering technique. Shashwat et al. proposed a segmentation method using the Fuzzy C-Means algorithm, employing extraction of tumor core using area and circulatory as criteria. A method was implemented by Nabizadeh et al. [20] in which they performed the automated segmentation for single spectrum MRI using the region-based segmentation approach. The whole research study covers in these aspects first is to extract the features to highlight the image textures, second proposed mechanism to reduce the less important features, third apply machine learning algorithms to classify images that have tumorous cells in them. To find the tumor contours they used Skippy greedy snake algorithm which helps to obtain the best results in accuracy are 93.8%. Integrating the dual-tree complex wavelet transform, a fully automated unsupervised brain MRI segmentation method was introduced by Jingdan Zhang et al. [30]. The research study used DT-CWT (Dual Tree Complex Wavelet Transform) and K-means algorithm for brain MRI segmentation and they

did the qualitative analysis. Clinical analysis for the brain tumor segmentation is still challenging task, due to the ambiguous tumor boundaries, Chaiyanan et al. [26] proposed a novel method in which a gray level co-occurrence matrix (GLCM) based on cellular automata was used for brain tumor segmentation. They introduced improved tumor cut (ITC) algorithm to get the high performance. State-of-the-art ITC and GLCM used for the segmentation and proposed model were evaluated using BRATS 2013 dataset with 0.84 DSC value.

Li, Yuhong et al. [16] proposed a technique based on the probabilistic model for the segmentation of multimodal brain MRI images. The solution for the spatial and structural variability in the segmentation problem in the referred technique combines two algorithms, i.e., Sparse Representation and Markov Random Forest. Nabizadeh et al. [19] proposed a fully automatic brain tumor segmentation method on MRI. The efficacy of the statistical features is evaluating the Gabor wavelet feature. Tom Haeck et al. [13] proposed a fully-automated method and this was the generative brain tumor segmentation method by Expectation-Maximization Approach. Soltaninejad Mohammadreza et al. [25] proposed the method using the superpixel-based extremely randomized trees. Extract texture based and structural based features. Superpixel-based segmentation applied and segment out the image into the number of patches. Support Vector Machine (SVM) and Extremely Randomized Tree (ERT) classifier used for classification between the normal and abnormal superpixels. The proposed model evaluated using BRATS 2012 dataset with SVM and ERT classifier, that obtained DSC 0.83 and 0.88 respectively. Rehman Zaka et al. [22] suggested superpixel based segmentation using statistical features, texton features based histogram, and fractal features. Feature selection and normalization has been applied using principal component analysis and independent component analysis. The proposed model evaluated by BRAST 2012 dataset and obtained 0.91 DSC.

Existing techniques are facing problems due to variation in tumor size, diversity in tumor shape and appearance. Recently, proposed solutions are discussed above which used statistical, textual, and curvature type features in tumor segmentation. Few of them used pixel-based, superpixel-based and region-based segmentation. Recent research methods in deep learning approaches to solve these tumor segmentation problems are also mentioned. The proposed model introduced an automatic technique to find the accurate tumorous area from brain MRI using superpixel-based segmentation with improved parameter values in superpixel segmentation. Different types of features such that statistical features, texton (Gabor) features, fractal features, curvature feature, and SIFT features have been extracted to get tumorous cells information. The reported approach also introduced a 'class balancing algorithm' to balance the feature vector obtained after feature extraction. By using this proposed algorithm enabled the model to have more accurate results. An ensemble technique has been introduced to get more accurate tumor area where we used SVM, Decision Tree, KNN and Ensemble classifiers to classify the superpixels based on the extracted feature values. DSC used as evaluation measure on the BRATS 2017 training dataset.

The proposed model has been divided into five main sections: the first section discussed brain MRI dataset with pre-processing techniques, the second section highlights the superpixel-based segmentation, the third section explain the feature extraction approaches, fourth section elaborate class balancing algorithm, and in fifth section classification between the normal and abnormal superpixels has been discussed.

2 The proposed methodology

The proposed model in an automatic detects and segment brain tumor abnormal tissues as shown in (Fig. 1) Proposed methodology has five main sections which are clearly defined below.

2.1 Preprocessing

Proposed model acquired open-source dataset known MICCAI BRATS 2017. It has both type of LGG and HGG volumes including T1-w, T2-w, T1c and FLAIR sequences and axial views. This training dataset total slices in one volume are 155 but few slices from start and few slices at the end are not have sufficient information. All these slices, which have lack of information are discarded by taking the mean value for all the slices in the dataset. All 3D slices have been converted into 2D format to feed into the model. Because the proposed model worked for the 2D slices.
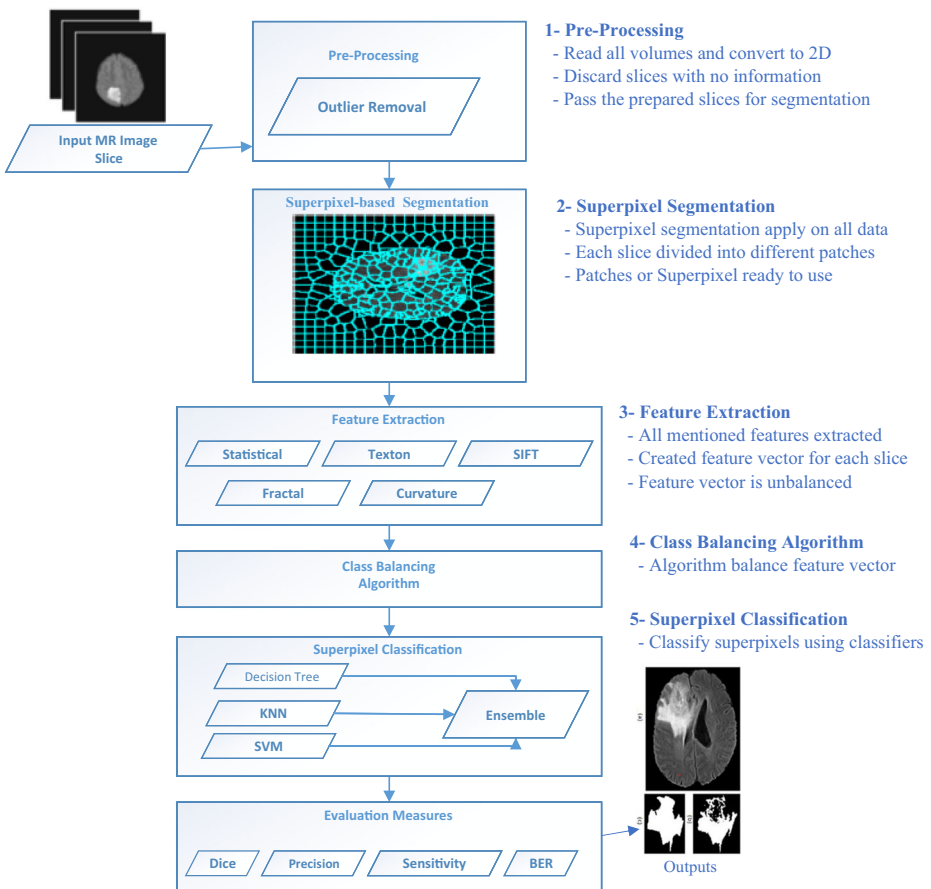

Fig. 1 The proposed model flow

2.2 Superpixel-Based segmentation

Simple Linear Iterative Clustering (SLIC) [1] algorithm is used to partition the images into approximately the equal size of patches. SLIC method has some parameters used to tune its algorithm to have more favorable results of segmentation. The boundary of the superpixel is defined by the spatial distance and the intensity distance. Moreover, it has very low computational cost and is an efficient in memory usage perspectives. In the proposed model, we choose the FLAIR sequence for evaluation of the proposed model. Every given slice is gridded into the approximately equal side size 'R', defined by the user. We represent grid size 'R' for these superpixels, and the geometrically center of the superpixel is also the center of the superpixel itself. On each iteration, these coordinates are updated based on intensity distance and spatial distance. Another parameter 'r' is there which known as the regularizer coefficient. The flexibility in all the superpixel boundaries is determined by regularizer r. More compact segments create when the regularizer r value high, and the segments create more flexible boundaries of the superpixels when the regularizer value low. To obtain the normalized intensity values the range is defined [25]. The detailed about the parameters tuned are discussed in the superpixel parameters section.

2.3 Feature extraction

We have extracted possible features in the proposed model using different image processing techniques. All the extracted features are mentioned in below sub-sections.

2.3.1 Intensity-based statistical features

The proposed model used grayscale images [24] and the intensity-based features [25] are extracted. In the grayscale images, the most important is a grey level which is distributed with different values in the selected region and these selected regions are known as superpixels. The details are discussed in the superpixel-based segmentation section. There is total 16 statistical features which are calculated listed: Angular second moment, Contrast, Correlation, Variance, Homogeneity, Sum Average, Sum Variance, Sum Energy, Entropy, Difference Variance, Difference Entropy, Information Measure of Correlation (I&II), Maximal Correlation Coefficient, Standard Deviation and Average.

2.3.2 Fractal features

Segmentation-based Fractal Texture Analysis (SFTA) [6] algorithm used to extract the fractal features, which is segmentation-based on the texture analysis. Otsu algorithm used to decompose the images into a set of binary images. These images (patches) are converted into binary images by multilevel thresholding. The thresholds represent by n_t and the value of n_t is defined as user required. In the proposed model the threshold values are set to n_t =2. All the image boundaries extracted by using edge detection [4] for each binary channel. The fractal feature extracts the area, intensity and fractal dimension from all these binary edge channels. To represent the number of all possible edge pixels in the selected superpixel which are known as area feature. As the mean intensity of the given image pixels which correspond to the edge pixels in the superpixel are known as intensity feature. The complexity in the structure of the
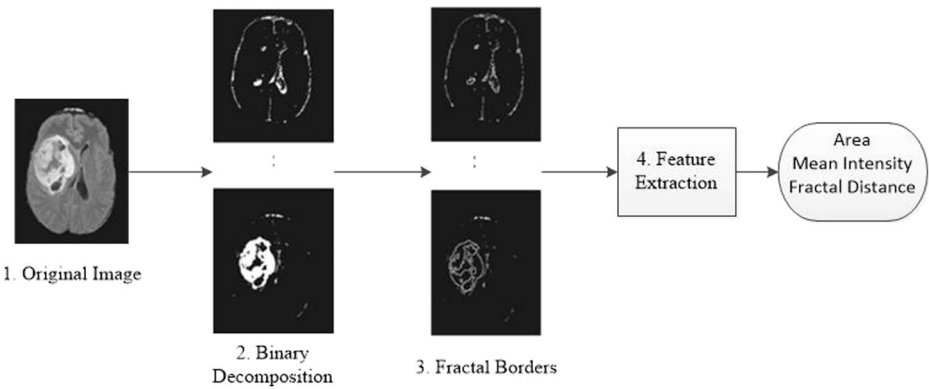
Fig. 2 Fractal features extraction flowchart

image, which is calculated from the boundaries of the image is known as the fractal dimension, and it is calculated as shown in the Eq. (1).

$$D_0 = \epsilon \rightarrow 0 \lim \frac{\log N(\epsilon)}{\log \epsilon^{-1}} \tag{1}$$

Where N (ϵ) represents the counting of hypercube of dimension E and length ϵ. By using the box-counting algorithm [23] an approximation of the fractal distance is obtained from the binary images. Figure 2 represents the flowchart for the extraction of fractal analysis only.

2.3.3 Texton features

The brain tissues are complex and have a complicated structure. Texture features are extracted to increase the accuracy of brain tumor segmentation. A specific filter bank produces texton after the convolution of the image, these textons are small elements of an image. Gabor filters [14] are used and discussed in Eq. (2).

$$G(x, y; \theta, \sigma, \lambda, \psi, \gamma) = exp\left(\frac{'x^2 + \gamma^{2'}y^2}{2\delta^2}\right) exp\left(i\left(2\pi\frac{'x}{\lambda} + \psi\right)\right) \tag{2}$$

Where σ is represented as the filter size, while the wavelength of the sinusoid is represented by λ, phase as the shift is denoted as ψ and spatial aspect ratio denoted as γ. The flow for texton features shown in Fig. 3.

2.3.4 Curvature feature

The image shape-based features are the curvature features and these features are calculated by taking the gradients along with the given directions such that x and y-direction are nominated by f_x and f_y. the most important is that image normal also calculated at the pixel (x, y) represent in the Eq. (3)^2.
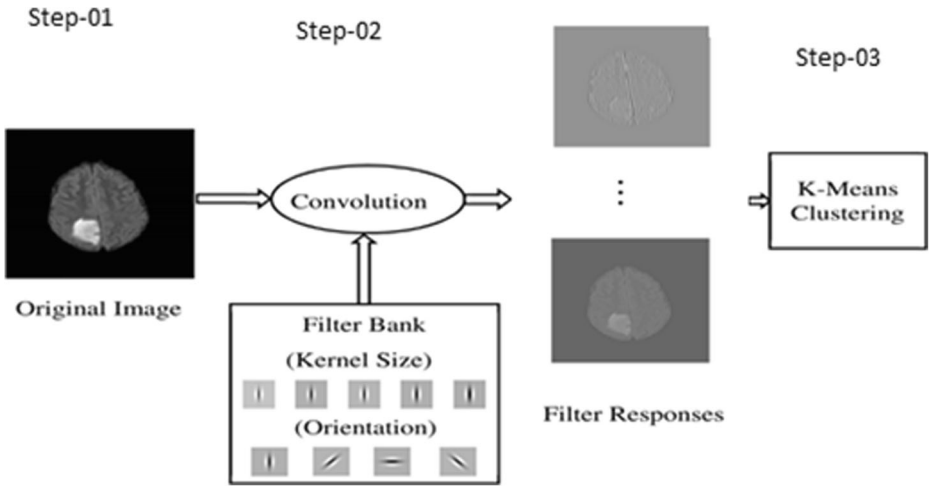
---

^{2} http://www0.cs.ucl.ac.uk/staff/ucacarr/teaching/ndsp/curvature.pdf.

Step-01

Step-02

Step-03

Original Image

Convolution

Filter Bank
(Kernel Size)

(Orientation)

Filter Responses

K-Means
Clustering

Fig. 3 Gabor filters applied to extract the texton features

$$\widehat{N}(x,y) = \frac{1}{\left(f_x^2 + f_y^2\right)^{1/2}} pmatrix f_x f_y pmatrix \qquad (3)$$

The divergence of the normal is the curvature of the 2D images and it is computed as shown in the Eq. (4).

$$Curv = \frac{f_{xx}f_y + f_{yy}f_x - 2f_{xx}f_xf_y}{\left(f_x^2 + f_y^2\right)^{3/2}} \qquad (4)$$

Where f_{xx} and f_{yy} are represented as the second derivatives and I (x, y) is denoted as the intensity of the image. When we take an average of all the curvature values for all those pixels in the superpixel is known as the curvature of each superpixel.

2.3.5 SIFT features

Scale-Invariant Feature Transform (SIFT) has two main parts one is to detect key points and another one is the keypoint descriptor. The detailed description of these paradigms is discussed.

For the SIFT features the first step is keypoint detection. To compute the SIFT features it's necessary to detect the key points which are calculated by the Degree of Gradient (DoG) and the image D (x, y, σ) after that L (x, y, σ) which represents the difference of smoothed images. Convolution applied of the given variable scale Gaussian with the given input image I (x, y) and resulted in L (x, y, σ) as represent in the Eqs. (5) and (6).

$$D(x,y,\sigma) = L(x,y,k\,\sigma) - L(x,y,\sigma) \qquad (5)$$

$$L(x,y,\sigma) = \frac{1}{2\pi\sigma^2} exp\left(-\frac{x^2 + y^2}{2\sigma^2}\right) *I(x,y) \qquad (6)$$

There are many DoG images obtained and it's performed between the different scales. Another aspect is that the local extremes which are detected from these DoG images by comparing 26

neighborhoods of a pixel within a set of three DoG images, and the pixel is represented as the key point if it is extremum [17].

The second point in the SIFT features is key point descriptor which is very important and gradient magnitude denoted as *m (x, y)* and *θ (x, y)* represents the orientation at each pixel in the smoothed image and the calculation shown in the Eqs. (7, 8 and 9) for key points:

$$m(x,y) = \sqrt{f_x(x,y)^2 + f_y(x,y)^2} \tag{7}$$

$$\theta(x,y) = \tan^{-1}\frac{f_y(x,y)}{f_x(x,y)} \tag{8}$$

$$\begin{cases} f_x(x,y) = L(x+1,y) - L(x-1,y) \\ f_y(x,y) = L(x,y+1) - L(x,y-1) \end{cases} \tag{9}$$

After that by the gradient magnitude, the weighted histogram of 36 directions is made and around the keypoint orientation in the region around, and the peak which assumed to be 80% and sometime it may be more for the maximum value of the histogram is assumed to be the orientation of the key point. And after giving some rotation to the given region around the key point to the orientation, at that point, the descriptor will be created.

2.4 Class balancing algorithm

A feature vector obtained after the extraction of features for each volume. These feature vectors are unbalanced like a large number of normal superpixels and very fewer amounts of abnormal. It needs to balance the feature vector. The proposed model introduced an algorithm to solve this problem, as shown below. The proposed model applies this algorithm and gets better results for classification. The proposed algorithm as shown as Algorithm 1, taking unbalanced feature vector '*F*' as input, after applying the random function on them and give output vector Ω. The output vector is used for the classification between normal and abnormal superpixels.

Algorithm 1: Class balancing algorithm
Input: F
[F= Feature vector]
Outputs: $\varnothing$, Ψ , Ω
[$\varnothing$ =class label one feature set
Ψ = class label zero feature set
Ω =balanced feature set]
Assume $\varnothing$ and Ψ empty lists.
For I =1 : size (F)
          If label(F) = 1
                    Append I to Ψ
          else
                    Append I to $\varnothing$
end For
for j= 1: size (Ψ)
          Ω_i = random with replacement ($\varnothing$)

2.5 Superpixel classification

In this phase we train the model using different classifiers such that SVM, KNN, Decision Tree and Ensemble classifier. After getting the trained model we classify the superpixels for each slice and these based on the superpixel feature values which obtained after feature extraction. Based on the feature values of each superpixel classified either normal or abnormal superpixel. The abnormal superpixel is basically tumorous area in the slice.

2.6 Evaluation measures

It is necessary to evaluate the developed model how well it's performed. The evaluation measures which we used to evaluate the proposed model performance is Dice Coefficient (DSC), Precision, Sensitivity and BER. The DSC evaluation parameter used for the evaluation of medical images, DSC is an overlap ratio between the segmented images from the proposed model and ground truths, the equation for DSC is shown in (10).

$$DiceCoefficient = \frac{2|X \cap Y|}{|X| + |Y|} \tag{10}$$

Sensitivity is defined as the number of all true positives, is the percentage of correctly classified positive examples among all examples, the truly signify the tumor pixels, sensitivity explained in Eq. (11).

$$Sensitivity = \frac{N_{TP}}{N_{TP} + N_{TN}} \times 100\% \tag{11}$$

Precision is the most common evaluation measure used, precision is the ratio of the brain pixels and the sum of truly represent the pixels of the brain and the falsely identified pixels of the brain. The formula to compute precision is shown in Eq. (12).

$$Precision = \frac{N_{TP}}{N_{TP} + N_{FP}} \times 100\% \tag{12}$$

Balanced Error Rate (BER) is an evaluation measure. BER used to check an average of the errors on each class, the formula for BER is shown in Eq. (13).

$$BER = 0.5 \left[\frac{N_{FP}}{(N_{TN} + N_{FP})} + \frac{N_{FN}}{(N_{FN} + N_{TP})} \right] \tag{13}$$

We used all these evaluation measures mentioned above to check the proposed model performance against the research problem statement.

3 Results and discussion

Experimental results of the proposed model are discussed in this section. The proposed model used MICCAI BRATS-2017 training dataset[3] [18] for testing and training purposes. There are some superpixel based segmentation parameters which we tuned for the experimental analysis.

---

[3] https://www.med.upenn.edu/sbia/brats2017/data.html.

In superpixels the region side size 'R' controls the region of any superpixel or patch as shown in Fig. 4. Whereas the regularizer 'r' controls the compactness of the patches as shown in Fig. 5. These parameters play an important role for the segmentation of images and if we pick large size superpixels then there is possibility for more than one classes in the single patch or superpixel, but if we set the size or take smaller size superpixel then there are less chances for more than one class in the superpixel. For this experiment we took different values for region side size 'R' as shown in the Fig. 4, where we took R = 5 value in case (b) but we took region side size R = 10 in the case (c), this experiment clearly shows there are chance of more than one class in the case (c) where we took region side size 'R = 10', because patches are bigger.

To check the effect of regularizer, 'r' which is varied but the region side size is kept constant (R = 10) as shown in Fig. 5. Regularizer is the parameter which used to check the optimum compactness of the superpixel or patch. We can see in Fig. 5 where the regularizer 'r' values impact on the image patches such that in the case (a) patches are not clear due to low 'r' value, case (b) due to increase in the 'r' value patches are more clear than previous case but these patches more visible in case (c) due to optimum value of the regularizer 'r'.

The effect of region side size 'R' by varying the superpixel size is shown in Fig. 6. The optimum superpixel size, i.e., 400, which produces better results than others are finalized after a number of experiments performed using MATLAB, has been selected.
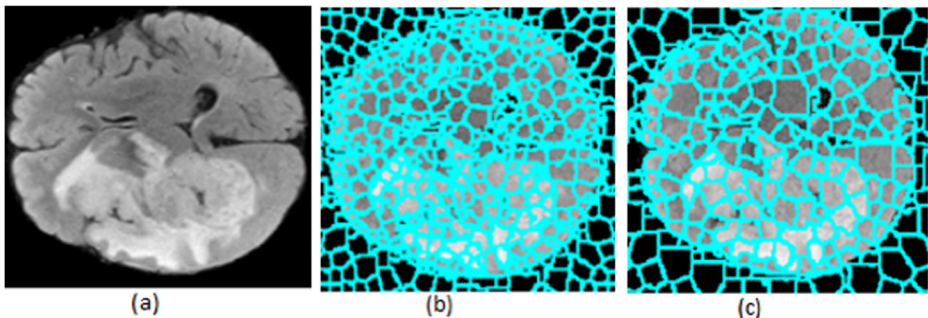

Fig. 4 Superpixel-based segmentation of slices with different region sizes 'R ' but same value for regularizer 'r': (**a**) Original image of FLAIR with High Grade Glioma (HGG) tumor (**b**) Region side size R = 5 and regularizer r = 0.2 (**c**) Region side size R = 10 and regularizer r = 0.2
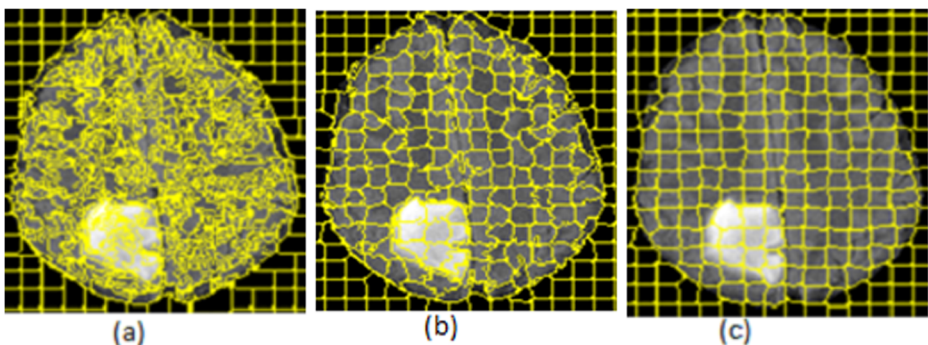

Fig. 5 Superpixel-based segmentation where R=10 (**a**) r=0, (**b**) r=0.2 and (**c**) r=0.5 are different compactness parameter
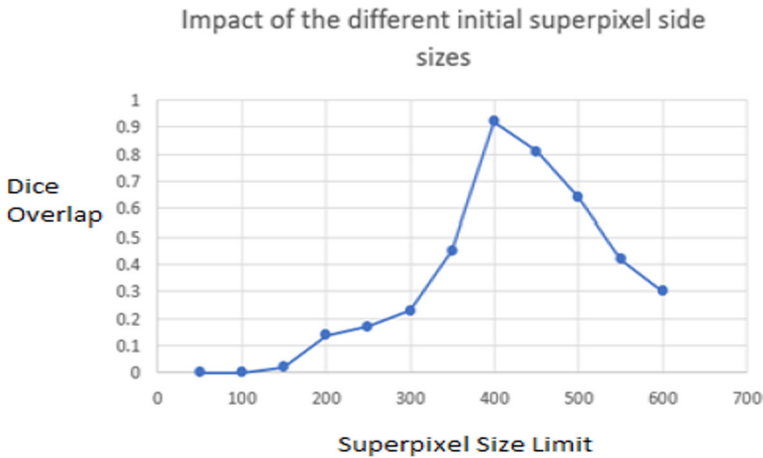
Fig. 6 Variation in the region side size 'R' and regularizer 'r' in superpixel segmentation

Figure 6 clearly shows the optimum size value for the superpixel with their tuned parameter values, at the very low values and very high values gives very bad dice coefficient values. The optimum value is 400 which gives best dice values results shown in the Fig. 6 graph. After various experiments and analysis finally we pick the superpixel value 400 for whole dataset of training and testing purposes.

3.1 Fractal features parameters

To extract the fractal features, there are several threshold levels applied to have optimum features. These features are used to check the threshold level for accuracy in the classification. Examined by increasing the threshold level n_t=2, these values create six binary channels and do not increase significantly by overlap measure. As we expand more levels, there is an increase of six more features (every binary channel creates a total three fractal features) in each feature vector. So, the threshold level for fractal feature extraction is chosen n_t=2, which gives optimum results for superpixel classification and feature extraction [25].

3.2 Texton features parameters

N_{FB} filter represents the total number of filters in the filter bank, has convolved all sequences. For each pixel, the response vector is created and the length of the vector are N_{FB}. As the number of pixels in the image is same, therefore, number of response vectors are clustered into the k-clusters and are calculated using k-means clustering. The response vector from the filter response, which is corresponding to each cluster considered as the texton of the texture class. In the end, the texton map is created by assigning the cluster number for each pixel. After that, for each superpixel, the texton features are calculated taking the histogram of the texton map.

Gabor filters are used to extract texton features in six directions, i.e., $[0^0, 30^0, 45^0, 60^0, 90^0, 120^0]$, while size and wavelength coefficient of Gabor filter, are selected empirically, which are 0.3, 1.5 respectively. Applying the k-means clustering algorithm on the different responses produced by these filters create texton maps [25].

3.3 Results analysis

The proposed model has been evaluated on MICCAI BRATS 2017 dataset [18], which consists of both High Grade Glioma (HGG) and Low Grade Glioma (LGG) volumes. HGG has 210 volumes, while LGG contains 75 volumes[4]. Although, each volume has four types of sequences, i.e., T1, T1Ce, T2, and FLAIR with its ground truth files. However, in this study, we utilized only FLAIR sequence. As FLAIR is the sequence having more contributing patterns for tumor region analysis [10]. The dataset is in the nifty files with extension ". nii", and has 3D data volumes. Each sequence is with 155 slices. Sample FLAIR sequence and its ground truth slice is shown in Fig. 7.

Normal and abnormal superpixels are classified using SVM, Decision Tree, KNN and an Ensemble classifier. Standard evaluation measures, i.e., Dice Coefficient (DSC), Precision, Sensitivity, and Balance Error Rates (BER) are used to evaluate the proposed model.

First of all, we evaluated the proposed model against each feature separately, the detailed average value for DSC is computed for each feature. DSC average value against statistical features, fractal features, texton features, curvature feature, and SIFT features are 0.52, 0.43, 0.68, 0.35, and 0.66 respectively. But this individual calculation of features couldn't play best role due to low DSC values.

After experimental analysis, we examined these individual features are not performing best, therefore, to check, which features combination performed the best, we employed the "leave one out" strategy. We did make all different possible combinations for the feature extraction. All the possible combination sets show with their optimum results, but when we combine all these features and used for the experiments it gives better results as compare to other sets, so we decide to use overall features for model training. We did experiment for LGG and HGG volumes both and the DSC values for all the combinations are shown in the Table 1. Statistical analysis on these feature combinations shows, when we combine all the features extracted and dice values greater than the other combination sets.

We used some machine learning classifiers, and check the model dice values by using these classifiers differently. We took SVM with their different kernels, Decision Tree, KNN and ensemble classifier individual to check which classifier performing better than others. But in all of them SVM with linear kernel has been used in this study, which obtained results closer to the ground truths as compare to other used classifiers. The results achieved on different classifiers are presented in Table 2. At the end we also did an experiment with ensemble technique where we combine all these classifiers and get the results based on maximum voting for the classifier.

We took some volumes for the experimental analysis as shown in the Table 2, and used SVM, Decision Tree, KNN and Ensemble classifier for the classification of normal and abnormal superpixels. After experimental analysis shown in Table 2, the SVM classifier and Ensemble got maximum DSC values as compare to the other classifiers. So, we choose this classifier for our model training and testing purposes.

3.4 Results for LGG segmentation

The visual results of LGG volumes are shown in Fig. 8. Figure 8(a) represents original image of LGG, Fig. 8(b) represents ground truth, Fig. 8(c) represents segmented image obtained
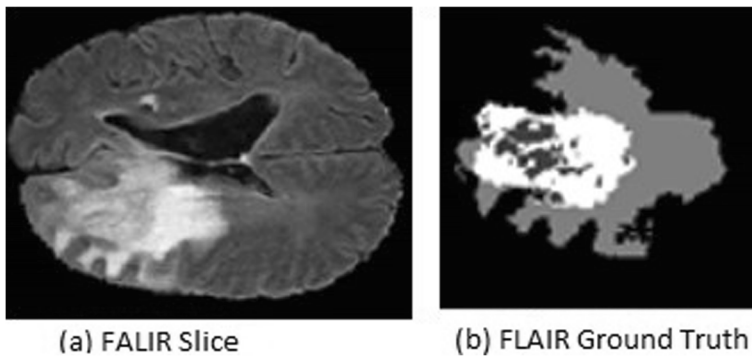
---

[4] https://www.med.upenn.edu/sbia/brats2017/data.html.

(a) FALIR Slice   (b) FLAIR Ground Truth

Fig. 7 MICCAI BRATS'17 training dataset (**a**) FLAIR slice (**b**) Ground Truth for the FLAIR slice

Table 1 Results of features leave-one-out strategy

Set No	Features Sets	LGG (DSC)	HGG (DSC)
1	Statistical, Texton, Fractal, and Curvature	0.80	0.81
2	Statistical, Texton, Fractal, and SIFT	0.70	0.71
3	Statistical, Texton, Curvature, and SIFT	0.70	0.71
4	Statistical, Fractal, Curvature, and SIFT	0.70	0.75
5	Texton, Fractal, Curvature, and SIFT	0.76	0.78
6	Statistical, Fractal, Texton, Curvature, and SIFT	**0.81**	**0.82**

through the proposed model, Fig. 8(d) represents original FLAIR image, Fig. 8(e) represents ground truth of Fig. 8(d) and (f) represent segmented image obtained through the proposed model.

Volume wise results obtained through the proposed model for LGG are shown in Table 3. Although, we evaluated the proposed model against each volume of the dataset, however, for ease of its representation, we represented results of every fifth volume in Table 3. 105 slices have been used for training, while 10 are used for testing of the proposed model. The maximum value obtained against all LGG volumes (average) as per DSC is 0.8593. To

Table 2 Results of different classifiers

Case No	SVM (DSC)	Decision Tree (DSC)	KNN (DSC)	Ensemble (DSC)
1	0.82	0.70	0.86	0.86
2	0.80	0.80	0.80	0.83
3	0.83	0.71	0.63	0.84
4	0.82	0.78	0.75	0.81
5	0.78	0.87	0.68	0.88
6	0.84	0.75	0.77	0.85
7	0.90	0.85	0.86	0.89
8	0.66	0.66	0.65	0.69
9	0.65	0.65	0.61	0.68
10	0.93	0.92	0.93	0.94
11	0.69	0.62	0.53	0.72
12	0.93	0.91	0.84	0.92
13	0.87	0.86	0.86	0.89
Mean	0.81±0.09	0.78±0.10	0.75±0.12	0.83 0.08
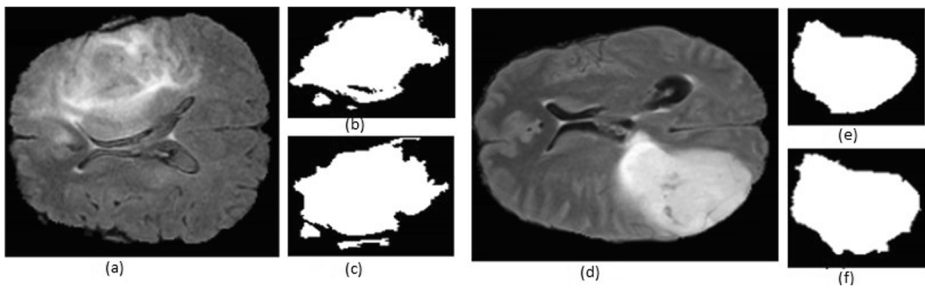
Fig. 8 Results of the proposed model for LGG volume, (**a**) Original Image (**b**) Ground Truth of (**a**), (**c**) Segmented Image of (**a**), (**d**) Original image, (**e**) ground truth of (**d**), (**f**) Segmented image of (**d**)

evaluate the proposed model in respect of its validation, precision, sensitivity, and BER achieved is 87.63%, 92.40% and 0.08 respectively.

Table 3 clearly shows the statistical results only for the LGG volumes, and these results shows our proposed model performance in the supervised learning approaches. Where we obtained these results using SVM and Ensemble classifier.

3.5 Results for HGG segmentation

The visual results of HGG volumes are shown in Fig. 9. Figure 9(a) represents original image of HGG, Fig. 9(b) represents ground truth of Fig. 9(a), (c) represents segmented image obtained through the proposed model, Fig. 9(d) represents original FLAIR image, Fig. 9(e)

Table 3 Comparison evaluation on superpixel classification using SVM classifier for LGG volumes

| Case No	Volume Name	Precision (%)	Sensitivity (%)	BER	DSC
1	Brats17_2013_6_1	78.24	91.00	0.17	0.9245
6	Brats17_2013_29_1	92.02	97.00	0.05	0.8541
11	Brats17_TCIA_241_1	93.31	96.00	0.06	0.9121
16	Brats17_TCIA_282_1	92.02	97.00	0.05	0.7401
21	Brats17_TCIA_639_1	85.01	89.00	0.06	0.9301
26	Brats17_TCIA_625_1	87.16	88.00	0.06	0.7821
31	Brats17_TCIA_462_1	80.28	86.00	0.07	0.8512
35	Brats17_TCIA_410_1	92.12	96.21	0.05	0.8802
Mean	All	87.63±0.6	92.40±0.5	0.08±0.04	0.8593±0.09
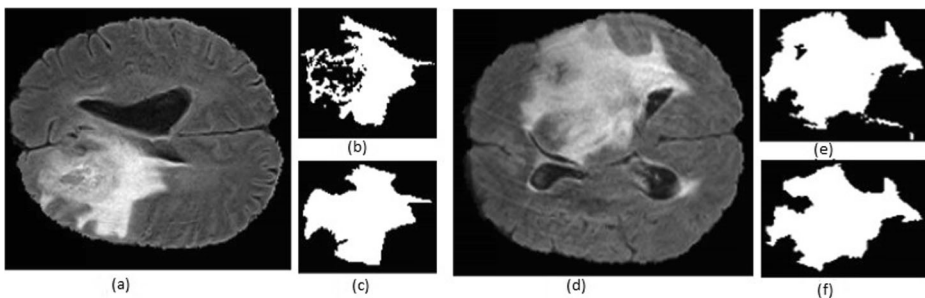
Fig. 9 Results of the proposed model for HGG volume representing (**a**) original Image (**b**) Tagged Image (**c**) Segmented Image (**d**) original image, (**e**) ground truth and (**f**) segmented image by model

represents ground truth of Fig. 9(d), and (f) represent segmented image obtained using the proposed model.

Volume wise results obtained through the proposed model for HGG are shown in Table 4. Although, we evaluated the proposed model against each volume of the dataset, however, for ease of its representation, we represented results of every fifth volume in Table 3. 105 slices have been used for training, while 10 are used for testing of the proposed model. The maximum value obtained against all HGG volumes (average) as per DSC is 0.8528. To evaluate the proposed model in respect of its validation, precision, sensitivity, and BER achieved is 87.03%, 97.74% and 0.08 respectively.

Table 4 statistical results against the HGG volumes, and all these results evaluated using SVM classifier with the linear kernel. Few volumes results are mentioned above on the five difference volumes only. The average DSC values for the HGG volumes are proved our proposed model performance.

3.6 Comparison with state-of-the-art studies

It is an important to compare the proposed model with state-of-the-art studies. Visual and statistical results obtained from proposed model is compared with state-of-the-art studies as shown in Tables 5 and 6. First, we have compared the reference paper DSC values for the same volumes that have used for their model evaluation. The reference paper used MICCAI BRATS-2012 and 2013 dataset volumes for model evaluation, whereas these same volumes are also available in the MICCAI BRATS-2107 training dataset that we used for our proposed model evaluation. Average DSC values for the proposed model on the same volumes is 0.82 while in reference paper [25], average DSC value is 0.80, which depicts that the proposed model outperformed as compared to the reference paper. The proposed model set the superpixel segmentation parameters with different experimental analysis, also introduce the class balancing algorithm for feature vectors and extract more features like SIFT which gives better results as compared to the reference paper [25].

Table 4 Comparison evaluation on superpixel classification using SVM-based classifier on BRATS 2017 dataset for HGG volumes

Case No	Volume Name	Precision (%)	Sensitivity (%)	BER	DSC
1	Brats17_2013_5_1	91.23	94.12	0.06	0.7965
6	Brats17_2013_22_1	87.16	92.00	0.09	0.8445
11	Brats17_2013_AQU_1	79.32	85.00	0.19	0.8985
16	Brats17_2013_ABO_1	93.31	96.00	0.06	0.8474
21	Brats17_2013_AMH_1	92.02	97.00	0.05	0.8124
26	Brats17_2013_AAG_1	79.02	87.00	0.08	0.8912
31	Brats17_CBICA_APY_1	92.02	97.00	0.05	0.7736
36	Brats17_CBICA_ASA_1	87.16	92.00	0.09	0.7941
41	Brats17_CBICA_AVJ_1	80.28	86.00	0.17	0.8524
46	Brats17_CBICA_AXO_1	85.34	88.00	0.06	0.8712
51	Brats17_TCIA_168_1	93.31	96.00	0.06	0.8645
56	Brats17_TCIA_211_1	93.31	96.00	0.06	0.9035
61	Brats17_TCIA_274_1	93.31	96.00	0.06	0.8542
66	Brats17_TCIA_374_1	87.12	89.00	0.06	0.8954
69	Brats17_TCIA_471_1	87.13	89.00	0.05	0.8924
Mean	All	87.03±0.5	97.74±0.5	0.08±0.05	0.8528±0.06

Table 5 Case by case comparison w.r.t DSC values with study [25]

Case No	Volume Name	Proposed Model (DSC)	Reference Paper (DSC)
1	Brats17_2013_6_1	0.92	0.84
2	Brats17_2013_8_1	0.75	0.88
3	Brats17_2013_15_1	0.85	0.78
4	Brats17_2013_5_1	0.74	0.74
5	Brats17_2013_7_1	0.88	0.78
6	Brats17_2013_10_1	0.65	0.65
7	Brats17_2013_12_1	0.84	0.88
8	Brats17_2013_14_1	0.85	0.86
9	Brats17_2013_22_1	0.84	0.84
10	Brats17_2013_26_1	0.86	0.75
11	Brats17_2013_27_1	0.83	0.81
Mean	All Volumes	0.82±0.07	0.80±0.07

Moreover, the results obtained through the proposed model have also been compared with the recent more state-of-the-art studies, which used MICCAI BRATS dataset, as shown in Table 6. It is evident that the average DSC value achieved in case of the results obtained using the proposed model is high as compare to the state-of-the-art studies.

Various techniques are introduced for this complex problem like tumor segmentation in brain MRI but there are need to address the spatial and intensity variation in the edema tumor, also in the tumor appearance. Hao Chen et al. [5] proposed solution to overcome the tumor segmentation problem in MRI using novel approach named Deep Convolutional Symmetric Neural Network (DCSNN), where they add more symmetry masks in the DCNN architecture layers, and they used BRATS 2015 dataset to evaluate the model where they obtained 0.852 DSC value and address the spatial variability of tumor in MRI. Linmin et al. [21] address the segmentation problem in brain MRI using two different approaches, feature fusion and joint label fusion (JLF). The purpose of this study was to find the accurate tumor segments in the BRATS 2015 MRI dataset, and this technique obtained average 0.85 DSC value. Accurately detection and segmentation for the brain is the need of time and there are various problems by using any manual method, Salma et al. [2] discussed about the novel approach using SegNet algorithm with the decision tree (DT) algorithm for classification of tumor. BRATS 2017 dataset used to evaluate the model and obtained 0.85 DSC/F-measure value. This fully automatic segmentation approach deal to overcome the various segmentation problems such that to give the solution for accurate segmentation of tumorous region.

Table 6 DSC results for the whole tumor/edema shows our proposed model outperformed as compare to the other state-of-the-art studies. The reason is that we used novel approach as discussed

Table 6 Comparison w.r.t dice co-efficient with state-of-the-art studies

Research Studies	Research Technique	DSC Values
Chen et al. [5]	DCSNN	0.8360
Chen et al. [5]	DCSNN+Postprocess	0.8520
Pei et al. [21]	Join Label Fusion (JLF)	0.8500
Pei et al. [21]	Random Forest (RF)	0.8520
Alqazzaz et al. [2]	SegNet_Max_DT	0.8500
Proposed Model	Superpixel-based	0.8593

in the research methodology and used large volume dataset for the better performance. There are some key points which helps in this study to improve the proposed model such that we used superpixel-based segmentation and tune the best parameters which perform best, extract various possible features like SIFT features, proposed class balancing algorithm for the unbalanced feature vector and used MICCAI BRATS 2017 whole dataset for the evaluation of proposed model.

4 Conclusions

This paper presented an automated segmentation of the tumor from brain MRI images using superpixel-based segmentation technique. To segment out the tumors from FALIR MRI pre-processing techniques applied to remove the outliers from slices, because it affects in the overall process. Superpixel-segmentation applied on the slices with the improved parameter values. In superpixel-based segmentation, the most important is the optimum size of the superpixel, in which the compactness parameter plays a vital role in the selection of the size of the superpixel. If the size of the superpixel is large, then more than one class will be available in the superpixel and result in false classification. Similarly, if the size of superpixel is small, then possible unique class is found. The optimum size of the superpixel has also been proposed in this study for better classification of tumors in brain MRI images. Several features including statistical, fractal, texton, curvature, and SIFT have been extracted. Due to large volume dataset and multiple features the obtained feature vector was unbalanced as it has larger number of normal class and small values of the abnormal class. The proposed model introduced class balancing algorithm to overcome this issue and different machine learning classifiers such that SVM, KNN, Decision Tree and ensemble have been used for training purpose. The proposed model has been evaluated on MICCAI BRATS-2017 training dataset using FLAIR modality. Evaluation measures, i.e., dice coefficient (DSC), precision, sensitivity, and BER results are 0.85, 87%, 97%, and 0.08 respectively evaluated both for segmentation and validation outcomes. Various existing techniques compared with the proposed model and our model outperformed due to the novel approach in superpixel segmentation parameters, class balancing algorithm and various new features. In future we can use large volume data with some deep learning techniques, and can give the practical application in real-time problem.

Declarations

Conflicts of interests/Competing interests We wish to confirm that there are no known conflicts of interest associated with this publication and there has been no significant financial support for this work that could have influenced its outcome.

References

1. Achanta R, Shaji A, Smith K, Lucchi A, Fua P, Süsstrunk S (2012) SLIC superpixels compared to state-of-the-art superpixel methods. IEEE Trans Pattern Anal Mach Intell 34(11):2274–2282
2. Alqazzaz S, Sun X, Yang X, Nokes L (2019) Automated brain tumor segmentation on multi-modal MR image using SegNet. Comput Vis Media 5:209–2192
3. Attique M, Gilanie G, Mehmood MS, Naweed MS, Ikram M, Kamran JA, Vitkin A (2012) Colorization and automated segmentation of human T2 MR brain images for characterization of soft tissues. PLoS One 7(3):e33616
4. Canny J (1986) A computational approach to edge detection. IEEE Transactions on pattern analysis and machine intelligence, pp 679–698

5. Chen H, Qin Z, Ding Y, Tian L, Qin Z (2020) Brain tumor segmentation with deep convolutional symmetric neural network. Neurocomputing 392:305–313
6. Costa AF, Humpire-Mamani G, Traina AJM (2012) An efficient algorithm for fractal analysis of textures. Paper presented at the 2012 25th SIBGRAPI Conference on Graphics, Patterns and Images
7. Elangovan A, Jeyaseelan T (2016) Medical imaging modalities: a survey. Paper presented at the 2016 International Conference on emerging trends in engineering, technology and science (ICETETS)
8. Ferlay J, Colombet M, Soerjomataram I, Parkin DM, Piñeros M, Znaor A, Bray F (2021) Cancer statistics for the year 2020: An overview. Int J Cancer 149(4):778–789
9. Gilanie G, Attique M, Naweed S, Ahmed E, Ikram M (2013) Object extraction from T2 weighted brain MR image using histogram based gradient calculation. Pattern Recognit Lett 34:1356–136312
10. Gilanie G, Bajwa UI, Waraich MM, Habib Z, Ullah H, Nasir M (2018) Classification of normal and abnormal brain MRI slices using Gabor texture and support vector machines. Signal Image Video Process 12:479–4873
11. Gilanie G, Bajwa UI, Waraich MM, Habib H (2019) Automated and reliable brain radiology with texture analysis of magnetic resonance imaging and cross datasets validation. Int J Imaging Syst Technol 29:531–5384
12. Gilanie G, Bajwa UI, Waraich MM, Habib Z (2019) Computer aided diagnosis of brain abnormalities using texture analysis of MRI images. Int J Imaging Syst Technol 29(3):260–271
13. Haeck T, Maes F, Suetens P (2015) Automated model-based segmentation of brain tumors in MR images. Proceedings BraTS Challenge 2015:25–28
14. Henriksen JJ (2007) 3D surface tracking and approximation using Gabor filters. South Denmark University, 28
15. Kadkhodaei M, Samavi S, Karimi N, Mohaghegh H, Soroushmehr SMR, Ward K, . . . Najarian K (2016) Automatic segmentation of multimodal brain tumor images based on classification of super-voxels. Paper presented at the 2016 38th Annual International Conference of the IEEE Engineering in Medicine and Biology Society (EMBC)
16. Li Y, Jia F, Qin J (2016) Brain tumor segmentation from multimodal magnetic resonance images via sparse representation. Artif Intell Med 73:1–13
17. Li W, Hosseini Jafari O, Rother C (2018) Deep object co-segmentation. Paper presented at the Asian Conference on Computer Vision
18. Menze BH, Jakab A, Bauer S, Kalpathy-Cramer J, Farahani K, Kirby J, Burren Y, Porz N, Slotboom J, Wiest R et al (2014) The multimodal brain tumor image segmentation benchmark (BRATS). IEEE Trans Med Imaging 34(10):1993–2024
19. Nabizadeh N, Kubat M (2015) Brain tumors detection and segmentation in MR images: Gabor wavelet vs. statistical features. Comput Electr Eng 45:286–301
20. Nabizadeh N, Kubat M (2017) Automatic tumor segmentation in single-spectral MRI using a texture-based and contour-based algorithm. Expert Syst Appl 77:1–10
21. Pei L, Bakas S, Vossough A, Reza SM, Davatzikos C, Iftekharuddin KM (2020) Longitudinal brain tumor segmentation prediction in MRI using feature and label fusion. Biomed Signal Process Control 55:101648
22. Rehman ZU, Naqvi SS, Khan TM, Khan MA, Bashir T (2019) Fully automated multi-parametric brain tumour segmentation using superpixel based classification. Expert Syst Appl 118:598–613
23. Schroeder M (2009) Fractals, chaos, power laws: Minutes from an infinite paradise. Courier Corporation
24. Sheela CJJ, Suganthi G (2019) Automatic brain tumor segmentation from MRI using greedy snake model and fuzzy C-means optimization. Journal of King Saud University-Computer and Information Sciences
25. Soltaninejad M, Yang G, Lambrou T, Allinson N, Jones TL, Barrick TR, Howe FA, Ye X (2017) Automated brain tumour detection and segmentation using superpixel-based extremely randomized trees in FLAIR MRI. Int J Comput Assist Radiol Surg 12(2):183–203
26. Sompong C, Wongthanavasu S (2017) An efficient brain tumor segmentation based on cellular automata and improved tumor-cut algorithm. Expert Syst Appl 72:231–244
27. Tan L, Ma W, Xia J, Sarker S (2021) Multimodal magnetic resonance image brain tumor segmentation based on ACU-Net network. IEEE Access 9:14608–14618
28. Yang T, Song J, Li L (2019) A deep learning model integrating SK-TPCNN and random forests for brain tumor segmentation in MRI. Biocybern Biomed Eng 39:613–6233
29. Zeineldin RA, Karar ME, Coburger J, Wirtz CR, Burgert O (2020) DeepSeg: deep neural network framework for automatic brain tumor segmentation using magnetic resonance FLAIR images. Int J Comput Assist Radiol Surg 15(6):909–920
30. Zhang J, Jiang W, Wang R, Wang L (2014) Brain MR image segmentation with spatial constrained k-mean algorithm and dual-tree complex wavelet transform. J Med Syst 38(9):1–6